Supporting Information for "Morphology of Jupiter's Polar Auroral Bright Spot Emissions via Juno-UVS Observations"

K. Haewsantati[1,2,3,4], B. Bonfond[1], S. Wannawichian [3,4], G. R. Gladstone[5], V. Hue[5], M. H. Versteeg[5], T. K. Greathouse[5], D. Grodent[1], Z. Yao[6,1], W. Dunn[7,8,9], J.-C. Gérard[1], R. Giles[5], J. Kammer[5], R. Guo[1], M. F. Vogt[10]

[1]LPAP, STAR Institute, Université de Liège, Liège, Belgium

[2]Ph.D. program in Physics, Department of Physics and Materials Science, Faculty of Science, Chiang Mai University, Chiang Mai, Thailand

[3]Department of Physics and Materials Science, Faculty of Science, Chiang Mai University, Chiang Mai, Thailand

[4]National Astronomical Research Institute of Thailand (Public Organization), Chiang Mai, Thailand

[5]Southwest Research Institute, San Antonio, Texas, USA

[6]Key Laboratory of Earth and Planetary Physics, Institute of Geology and Geophysics, Chinese Academy of Sciences, Beijing, China

[7]Mullard Space Science Laboratory, Department of Space and Climate Physics, University College London, Dorking, UK

[8]The Centre for Planetary Science at UCL/Birkbeck, London, UK

[9]Harvard-Smithsonian Center for Astrophysics, Smithsonian Astrophysical Observatory, Cambridge, MA USA

[10]Center for Space Physics, Boston University, Boston, MA, USA

Contents of this file

Additional Supporting Information (Files uploaded separately)

1. Captions for large Table S1

Introduction

The supporting information materials are following.

1. The histogram shows the distribution of the solar zenith angles of bright spots which represent the relation between the bright spot occurrence and the exposure to the sunlight.

2. We show the polar projection of bright spots and the SIII longitude position after extrapolation to location that can be mapped by Vogt's mapping model.

3. The color ratio plot shows bright spot detected during PJ1 in high color ratio region.

4. We also show the power variation for PJ4 which has quasiperiodic behaviors as same as the PJ16 power variation plot (Figure 6.)

5. Based on period analysis using Lomb-Scargle periodogram method for bright spots during PJ4 and PJ16, the Lomb Normalized Periodogram will be presented.

References

Bonfond, B., Gladstone, G. R., Grodent, D., Greathouse, T. K., Versteeg, M. H., Hue, V., ... Kurth, W. S. (2017, May). Morphology of the UV aurorae Jupiter during Juno's first perijove observations. *Geophysical Research Letters*, *44*(10), 4463–4471. Retrieved 2019-02-25, from https://agupubs.onlinelibrary.wiley.com/doi/full/10.1002/2017GL073114 doi: 10.1002/2017GL073114

Bonfond, B., Saur, J., Grodent, D., Badman, S. V., Bisikalo, D., Shematovich, V., ... Radioti, A. (2017, August). The tails of the satellite auroral footprints at Jupiter. *Journal of Geophysical Research: Space Physics*, *122*(8), 7985–7996. Retrieved 2018-08-31, from https://agupubs.onlinelibrary.wiley.com/doi/abs/

10.1002/2017JA024370 doi: 10.1002/2017JA024370

Connerney, J. E. P., Kotsiaros, S., Oliversen, R. J., Espley, J. R., Joergensen, J. L., Joergensen, P. S., ... Levin, S. M. (2018, March). A New Model of Jupiter's Magnetic Field From Juno's First Nine Orbits. *Geophysical Research Letters*, *45*(6), 2590–2596. Retrieved 2018-10-25, from https://agupubs.onlinelibrary.wiley.com/doi/abs/10.1002/2018GL077312 doi: 10.1002/2018GL077312

Vogt, M. F., Bunce, E. J., Kivelson, M. G., Khurana, K. K., Walker, R. J., Radioti, A., ... Grodent, D. (2015, April). Magnetosphere-ionosphere mapping at Jupiter: Quantifying the effects of using different internal field models. *Journal of Geophysical Research: Space Physics*, *120*(4), 2584–2599. Retrieved 2018-08-30, from https://agupubs.onlinelibrary.wiley.com/doi/abs/10.1002/2014JA020729 doi: 10.1002/2014JA020729

Vogt, M. F., Kivelson, M. G., Khurana, K. K., Walker, R. J., Bonfond, B., Grodent, D., & Radioti, A. (2011, March). Improved mapping of Jupiter's auroral features to magnetospheric sources. *Journal of Geophysical Research: Space Physics*, *116*(A3). Retrieved 2019-02-25, from https://agupubs.onlinelibrary.wiley.com/doi/full/10.1029/2010JA016148 doi: 10.1029/2010JA016148

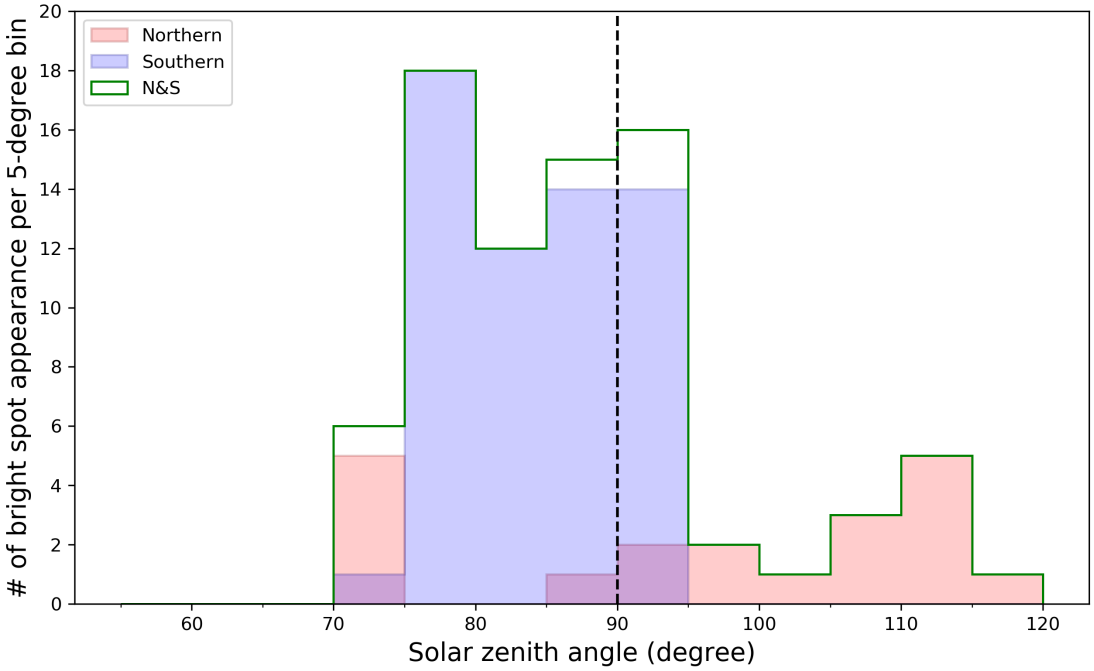

Figure S1. Distribution of solar zenith angles of bright spots in Northern hemisphere (pink), Southern hemisphere (blue), and the combined spots from both hemispheres (green line). The dashed vertical line represents 90°zenith angle at which the sun is on the horizon. The angles larger than 90°refer to the case that the sun is below the horizon, corresponding to the night time.

Table S1. The bright spot characteristics observed during PJ1 to PJ25 are presented. The power is calculated from the total brightness in bright spot's elliptical area. This power is different from the power variation plot (Figure 6 and Figure S4) which is the integrated area corresponding to all bright spots detected during a perijove. The last two columns are mapped positions in magnetosphere and the local times from Vogt's magnetic flux equivalent using JRM09 model.

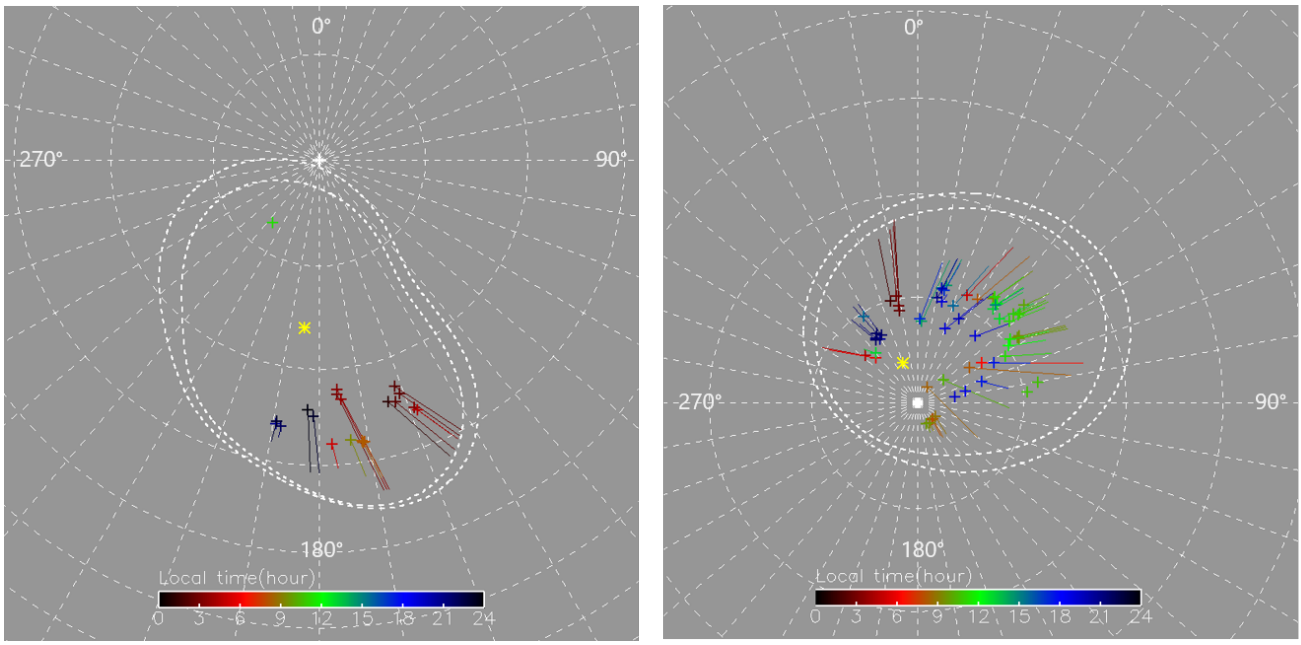

Figure S2. Polar projections (Left: Northern, right: Southern) show positions of bright spots and local times according to Vogt's magnetic flux equivalent mapping with JRM09 model. The grid represents meridians and parallels in the SIII jovi-centric system, spaced every 10°. The two dash contours are the statistical locations of the main emission for the compressed and expanded cases (Bonfond, Gladstone, et al., 2017). The yellow asterisk represents the magnetic pole of each hemisphere (Bonfond, Saur, et al., 2017; Connerney et al., 2018). The lines represent the tracing paths from the magnetic pole to the bright spots' peak positions in the directions toward system III longitudes and latitudes, which can be mapped by Vogt's mapping model.(Vogt et al., 2011, 2015)

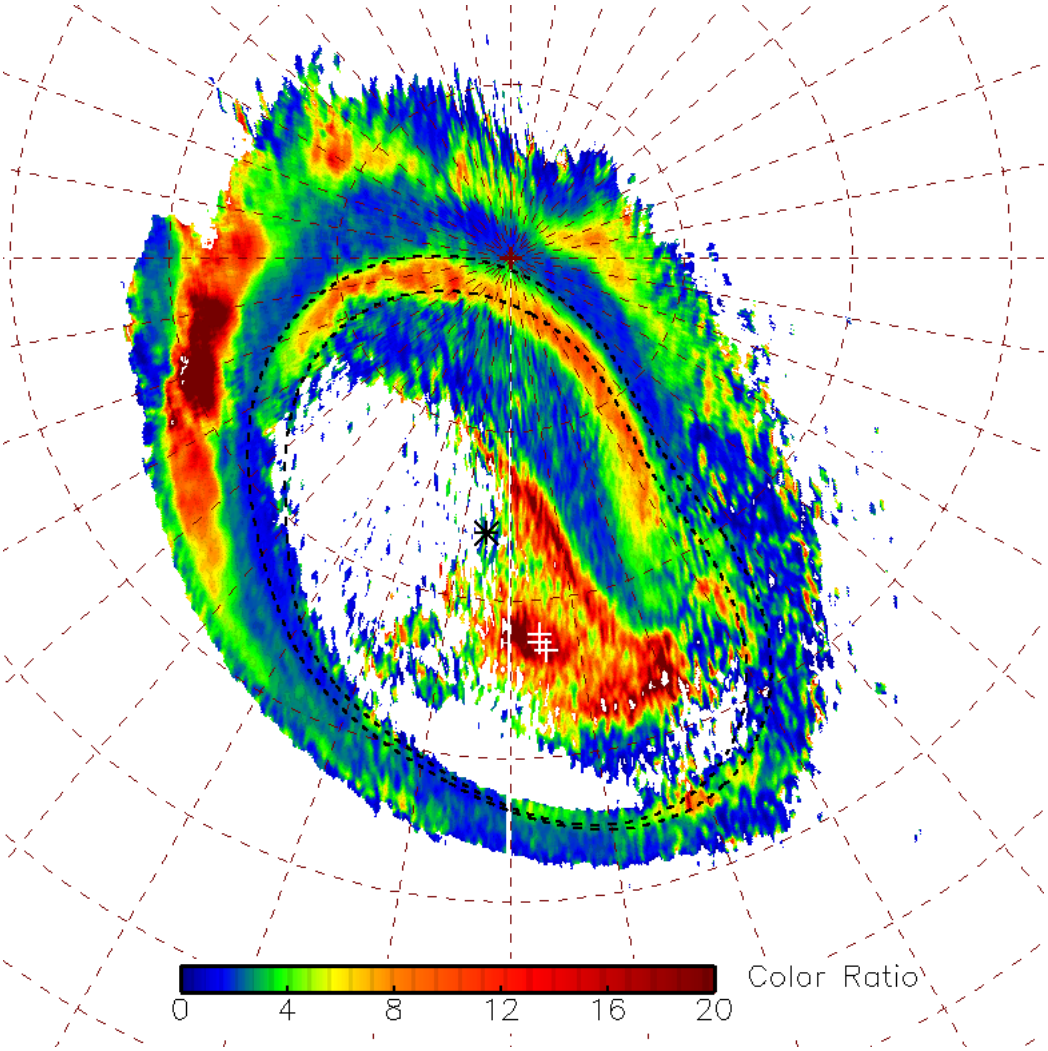

Figure S3. The color ratio map observed from PJ1 shows the bright spots positions (plus symbols) in high color ratio region. The asterisk represents the magnetic pole. The grid coordinates and two dashed contours are the same as in figure S2.

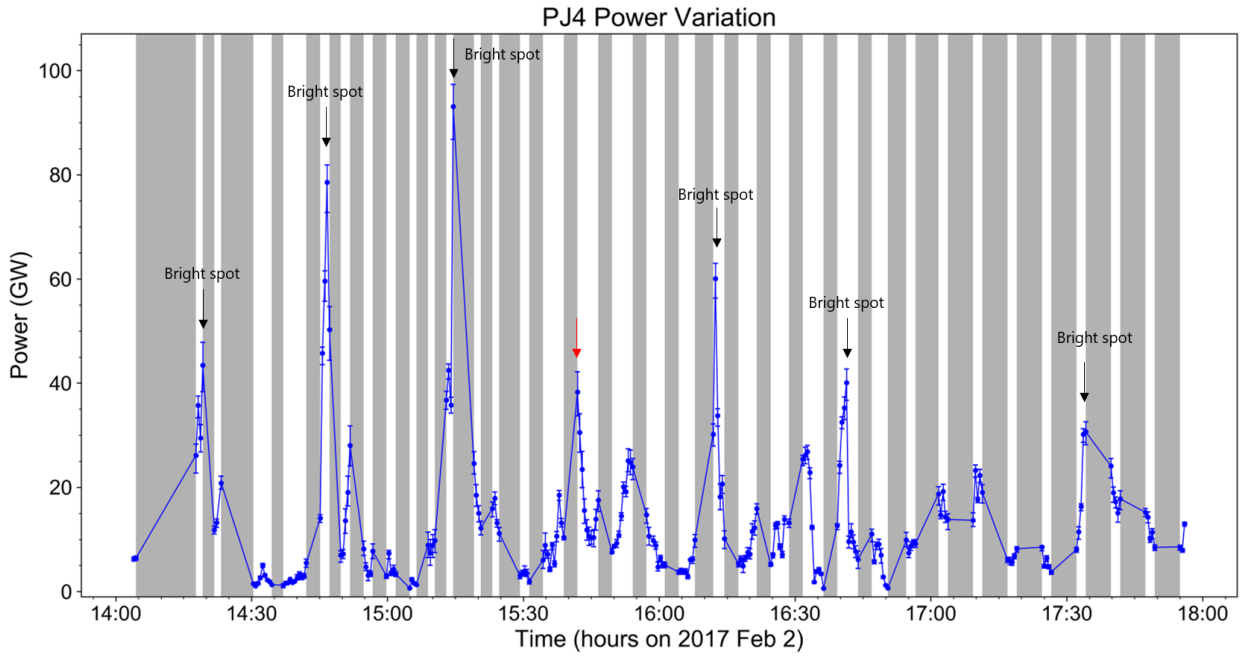

Figure S4. The power variation as a function of time for the southern bright spots during PJ4. The black arrows indicate the times that bright spots appear in UVS view. The red arrow presents the peak at which no bright spot appears but there is the increase in the brightness in the region of interest. The grey areas indicate times when the region of interest is covered by UVS view less than 50%.

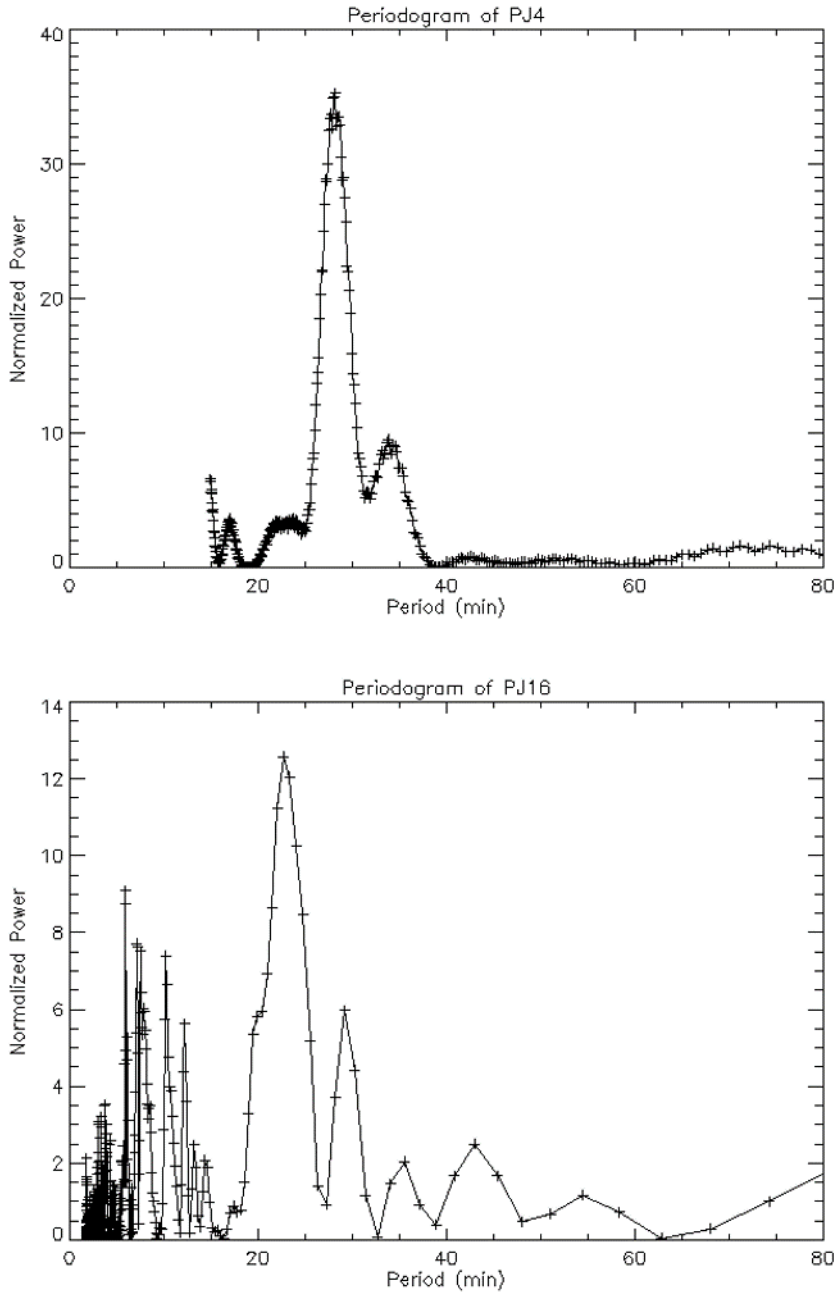

Figure S5. Fitted result from Lomb-Scargle periodogram for PJ4 (top) and PJ16 (bottom). The dashed lines represent significant levels. The lower significant level implies the high probability for the period to be important. The highest peak of normalized power for PJ4 corresponds to period 28.18 minutes. In addition, for PJ16, the clearest peak of normalized power in our period range is 22.68 minutes.